Numerical Prediction of Convective Heat Transfer in Self-Sustained Oscillatory Flows

Cristina H. Amon*
Carnegie Mellon University, Pittsburgh, Pennsylvania
and
Bora B. Mikic†
Massachusetts Institute of Technology, Cambridge, Massachusetts

Numerical investigations of the flow pattern and heat transfer enhancement in supercritical grooved-channel and communicating-channels flows are presented. For Reynolds numbers above the critical one, $R_c = 0(100)$, these flows exhibit laminar self-sustained oscillations at the plane channel Tollmien-Schlichting frequency. These ordered, very well-mixed flows require significantly less pumping power than the random fluctuating turbulent flows to achieve the same transport rates. Comparing different heat transfer augmentation schemes in grooved channels, it is shown that the best enhancement system regarding minimum power dissipation corresponds to passive flow modulation in the range of low Nusselt numbers. However, spontaneous supercritical flow destabilization becomes competitive as the Nusselt number is increased. It is found that on an equal pumping power basis, the heat transfer in communicating channels flows is up to 300% higher than the one in flat channel flow.

Nomenclature

a = groove depth (Fig. 1)
D = computational domain
f = pressure gradient
h = half-channel height (Fig. 1)
k = thermal conductivity
L = periodicity length
ℓ = groove width (Fig. 1)
Nu = Nusselt number, $q''_0 h/k\Delta\bar{T}$
P = pressure
Pr = Prandtl number, ν/α
Q = flow rate
q'' = heat flux per unit area
q''_0 = heat flux per projected area
R = Reynolds number, (3/2) Vh/ν
T = temperature
t = time
u,v = velocity components in the x- and y- directions, respectively
V = time-mean, channel-averaged velocity
v = vector velocity
α = thermal diffusivity
$\bar{\Delta}T$ = time- and space-averaged temperature difference between wall and mixed mean fluid temperatures
∂D = boundary of D
Φ = nondimensional pumping power defined by Eq. 12
θ = periodic temperature
ν = kinematic viscosity
ξ = periodicity index
Π = dynamic pressure
ρ = density
σ = decay rate
ω = vorticity
ω = angular frequency

Subscripts
a = adiabatic
c = critical
h = heat flux
p = periodic
s = solid wall
TS = Tollmien-Schlichting
t = time derivative

I. Introduction

APPLICATIONS such as cooling of modern electronic components, mass transport in biomedical devices, and heat transfer in compact plate-finned heat exchangers have created an increasing interest in transport enhancement schemes in small size systems with moderate Reynolds number flows. The evaluation and comparison of different augmentation schemes must consider, in addition to the increase in transport rates, the penalty associated with the increase in dissipation and pumping power.

An important aspect of transport enhancement is the mixing produced by hydrodynamic instabilities. Systems that exploit this feature require a separated flow region that produces inflexional velocity profiles susceptible to inviscid destabilization which, in turn, lead to significant convective motions responsible for the transport enhancement. These separated flow systems are capable of subcritical destabilization either by imposing externally an oscillatory flow (active modulation)[1,2] or by inserting eddy promoters (passive modulation).[3,4] In the first case, the flow is modulated at the system least-stable natural frequency in order to get resonant behavior. However, supercritical destabilization is achieved naturally in periodic inhomogeneous geometries when the separated flow system operates above a certain critical Reynolds number R_c. In this regime, the flow presents a time-periodic behavior with laminar self-sustained oscillations at a well-defined frequency. The R_c for the onset of oscillations, which depends strongly on the geometric parameters,[5] is typically lower than the Reynolds number for transition to turbulent flow.[6] This is in agreement with the nonrigorous application of Squire's theorem, according to which the first instability to set in is two dimensional.[7]

In this study, we analyze two different periodic configurations: the grooved-channel geometry (Fig. 1a) as a model for

Received Dec. 19, 1988; revision received July 10, 1989.

*Assistant Professor, Department of Mechanical Engineering. Associate Member AIAA.
†Professor, Department of Mechanical Engineering.

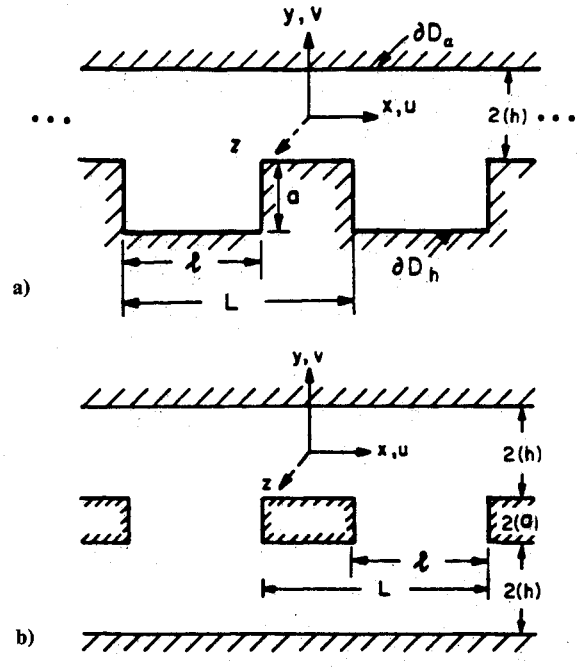

Fig. 1 Typical geometries, periodic in the streamwise x direction and infinite in z direction: a) grooved channel b) communicating channels.

an array of chips located on a circuit board[8] and the communicating channels geometry (Fig. 1b) as representative of compact plate-finned heat exchangers with perforated or slotted fins.[9,10] Heat-transfer surfaces, periodically interrupted along the streamwise direction, have been widely used to improve the performance of heat exchange devices and therefore reduce their sizes. Such an arrangement may be viewed as a succession of colinear plate segments aligned parallel to the flow, with gaps between successive plates (Fig. 1b). Each gap enables the interruption of the thermal boundary layer where the highest resistance to the heat flux occurs and the restarting of a new one with lower thermal resistance. Furthermore, it promotes very good mixing of the flow with self-sustained oscillations when the system is operating above critical conditions.

Along with the augmentation of the heat transfer coefficient, there is an increase in pressure drop because of 1) the higher skin friction associated with the successive boundary layer restartings and 2) the creation of separated flow regions. Therefore, the evaluation of the overall performance should take into account the pressure drop and pumping power as well as the enhanced heat transfer coefficient.

In an enhancement problem formulated as follows: "For a given fluid, channel height and a required value of Nusselt number, determine the flow Reynolds number and geometric parameters that would yield minimum pumping power," it can be shown by applying the classical Reynolds' analogy[11,12] that in well-mixed flows, viscous dissipation scales linearly with the Nusselt number and quadratically with the Reynolds number. This implies that a flow that achieves a given transport rate at lower Reynolds number will have less viscous dissipation requiring less pumping power. Therefore, from the preceding optimization criterion, "an optimal heat transfer system is equivalent to a more unstable system, i.e., a system with lower critical Reynolds number R_c," where R_c refers to the Reynolds number for the onset of laminar oscillations.

In this paper, the incompressible flow in periodic grooved-channel and communicating channels is investigated by direct numerical simulation. The conclusion drawn with the use of the classical Reynolds' analogy is also verified, showing that these very well-mixed, oscillatory, but still laminar flows require less pumping power than turbulent flows to achieve comparable transport rates. In Sec. II, the mathematical problem is formulated, and the numerical technique is briefly described. In Sec. III, solutions for subcritical steady-flows are presented, that provides a baseline to which the supercritical flows can be compared. In Sec. IV, the flow patterns for self-sustained oscillatory flows in grooved-channel and communicating channels are analyzed. Finally, in Sec. V, pumping power and the Nusselt number for supercritical flows are computed. Comparisons are made with the results for plane channel flow, eddy promoters, and externally modulated flows.

II. Mathematical and Numerical Formulation

The geometries to be considered (see Fig. 1) are periodic in the streamwise x-direction and infinite in the spanwise z-direction. The flow is assumed to be fully developed in x, and independent of z.

The governing equations for incompressible flow are the Navier-Stokes, mass conservation, and energy equations written in primitive variables as

$$v_t = vx\omega - \nabla\Pi + R^{-1}\nabla^2 v, \qquad \text{in } D \tag{1}$$

$$\nabla \cdot v = 0, \qquad \text{in } D \tag{2}$$

$$T_t + \nabla \cdot (vT) = (R.Pr)^{-1}\nabla^2 T, \qquad \text{in } D \tag{3}$$

where $\Pi = p + |v|^2/2$ is the dynamic pressure. The flow is also governed by the geometric parameters a, ℓ, and L. This problem is nondimensionalized by scaling the velocities by $3/2V$ and the lengths by one channel half-height h. The temperature is nondimensionalized by $q''h/k$, where q'' is the uniform flux imposed at the wall.

The fully developed boundary conditions for the velocity field are

$$v(x,y,t) = 0 \qquad \text{on } \partial D_s \tag{4a}$$

$$v(x + \zeta L, y, t) = v(x,y,t) \qquad \text{on } \partial D_p \tag{4b}$$

corresponding to no-slip and periodicity of the fully developed flow in the x direction where ζ is an integral periodicity index. The pressure can be decomposed as follows

$$\Pi(x,y,t) = -\frac{dp}{dx}(t)x + \tilde{\Pi}(x,y,t) \tag{5a}$$

$$\tilde{\Pi}(x + \zeta L, y, t) = \tilde{\Pi}(x,y,t) \tag{5b}$$

where $dp/dx(t)$ is the driving pressure gradient, which is determined indirectly by the imposed flow-rate condition,

$$Q = \int u(x = 0, y, t)\, dy = 4/3 \tag{6}$$

The linear pressure term in Eq. (5a) is consistent with periodicity of the velocity of Eq. (4b), since only the gradient of the pressure appears in Eq. (1).

The thermal boundary conditions are uniform heat flux and adiabatic surface,

$$\nabla T \cdot \hat{n} = q''/k \qquad \text{on } \partial D_h \tag{7a}$$

$$\nabla T \cdot \hat{n} = 0 \qquad \text{on } \partial D_a \tag{7b}$$

where $\hat{n}$ is the outward normal on the domain boundary.

For periodic, thermally developed domains, the temperature can be decomposed into a linear part and a periodic contribution,

$$T(x,y,t) = \theta(x,y,t) + \gamma x \tag{8a}$$

$$\theta(x + \zeta L, y, t) = \theta(x,y,t) \tag{8b}$$

where $\gamma = q'/R\,Pr\,Q\,L$ and q' is the total heat transfer rate into the domain. In order to obtain the appropriate periodic condition for θ, a linear term is subtracted to compensate for the rise in mixed-mean temperature because of the net heat flux input.

Numerical Method

The numerical approach followed here is that of direct simulation, in which the system [see Eqs. (1-8)] is solved using initial value solvers. In particular we find steady states through time evolution, we calculate the linear stability of these steady or unsteady states, and we follow the nonlinear evolution and saturation of the resulting flows, using the same type of initial value solvers.

The temporal discretization of the governing equations is performed using a multistep fractional scheme.[13] The convective nonlinear term is marched in time using a third-order Adams-Bashforth scheme, and the pressure and diffusion contributions are treated implicitly applying the Euler Backward or Crank-Nicolson schemes.

The spatial discretization of the computational domain proceeds using the spectral element method.[14,15] This is a high-order, weighted-residual technique that exploits both common features and the competitive advantages of low-order finite-element methods (generality and geometric flexibility) and the p-type spectral techniques (accuracy and rapid convergence). In the spectral element discretization, the computational domain is divided into general quadrangular macro-elements. Within each element, the dependent and independent variables are represented in terms of high-order, tensor-product polynomial expansions through Chebyshev collocation points. Mixed variational and collocation operators are used to generate the discrete equations with interfacial continuity constraints imposed naturally via variational statements; this approach results in a weak coupling between the dependent variables in adjacent elements and relative sparse matrices, making the method efficient and easy to implement. Spectral methods have proven to be a very powerful tool for analyzing fluid flows and heat transfer because of their ability to represent accurately the thermo-fluid variables and resolve high local gradients with fewer grid points. Using spectral element methods, we have simulated accurately highly unsteady two-dimensional laminar flows with heat transfer.[1,16] Therefore, this technique is well suited for the purpose of this work.

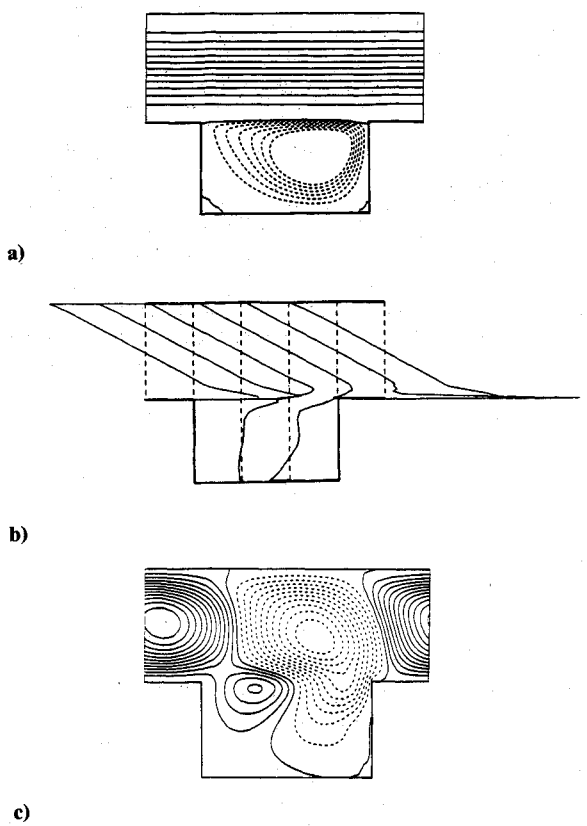

Fig. 2 Grooved-channel steady flow at $R = 250$ a) streamlines b) $\partial u/\partial y$, the dashed lines indicate the x location of the plot as well as the zero reference for $\partial u/\partial y$, c) instantaneous streamlines of the decaying least-stable perturbation mode.

III. Subcritical Steady-State Flows

The numerical results presented here are obtained by direct simulation of Eqs. (1-8) iterating in time for arbitrary initial conditions until a stable steady or periodic state is found. The base geometries, shown in Fig. 1, have a nondimensionalized

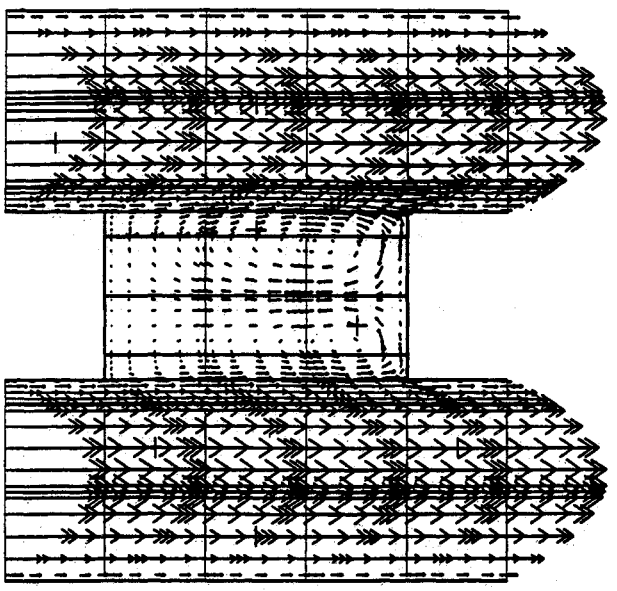

Fig. 3 Velocity vectors of the steady communicating channels flow at $R = 80$. (Two counter-rotating vorticities are aligned and confined in the groove.)

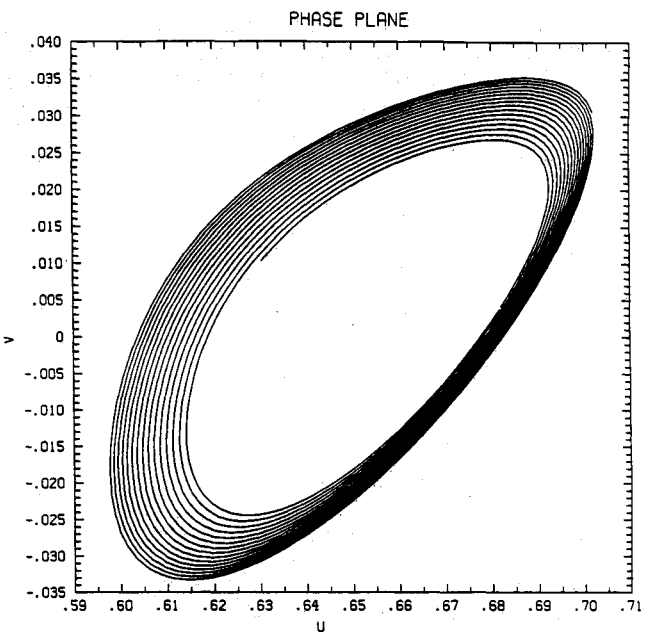

Fig. 4 Phase plane portrait of v vs u as it is approaching a limit cycle, at $R = 400$.

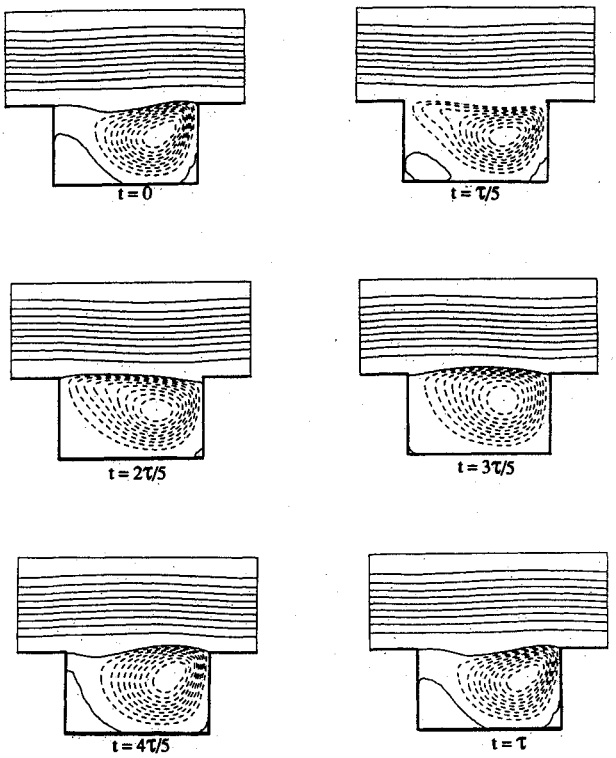

Fig. 5 Instantaneous streamlines at six times during one cycle of the self-sustained oscillatory flow at $R = 400$.

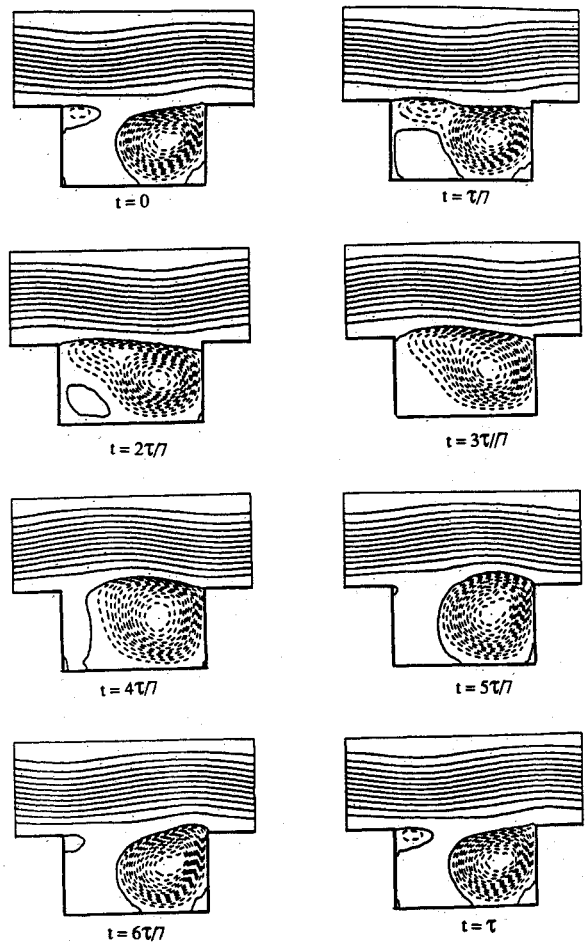

Fig. 6 Instantaneous streamlines at eight times during one cycle of the self-sustained oscillatory flow at $R = 700$. The groove vortex is seen to be ejected during the cycle.

periodicity length $L/h = 5$ and groove width $\ell/h = 3$. The ratio of the groove-to-channel height is $a/h = 1.68$ (see Fig. 1a), and the nondimensionalized separation between channels, is $2a/h = 1.0$ and 1.68 (see Fig. 1b).

A. Grooved Channel

The streamlines for the grooved-channel steady flow at $R = 250$ are presented in Fig. 2a. They show a separated flow region with a large-scale recirculating vortex which is responsible for the creation of a strong velocity inflexion point. This is clearly seen in Fig. 2b by a plot of the steady $\partial u/\partial y$ profiles at different x locations of the grooved channel, where the inflexion point corresponds to the maximum of $\partial u/\partial y$. This contrasts with plane Poiseuille flow whose parabolic "laminar" profile is inviscidly stable due to the lack of inflexion point. The critical Reynolds number for the onset of unsteadiness in grooved channel is much lower than that for plane Poiseuille, although it depends strongly on the relative dimensions of the grooved-channel geometry.[5]

However, in spite of this low critical Reynolds number and strong inflectional point, the stability modes are similar to traveling channel Tollmien-Schlichting waves (TS) as shown in Fig. 2c, by a plot of stable linear perturbation streamlines at $R = 250$; moreover, any perturbation imposed to the steady flow decays with a frequency very close to that corresponding to the least stable plane Poiseuille mode.[6,17]

B. Communicating Channels

For the communicating channels geometry, the steady-state field is shown in Fig. 3 in the form of velocity vectors for Reynolds number $R = 80$. Two counter-rotating vortices are aligned and confined in the groove. There is almost no communication between the groove and core flows. This is clearly seen from the velocity profile in the channel part which is very close to a parabolic plane-Poiseuille-flow profile.

A time-asymptotic result for the convergence of the streamwise velocity to its steady-state value at $R = 100$ shows that the least stable mode is oscillatory with a decay rate and angular frequency of $\sigma = -0.01439$ and $\omega = 0.653$, respectively, where the frequency is nondimensionalized by the convective time. Notice that for a plane channel wave corresponding to the same wave number, the decay rate and frequency are $\sigma_{TS} = -0.1682$ and $\omega_{TS} = 0.652$. Therefore, the frequency of the decaying mode is very close to the Tollmien-Schlichting frequency corresponding to the same spatial structure of *one* channel, whereas the decay rate indicates the destabilizing effect of the channel communication.

IV. Supercritical Self-Sustained Oscillatory Flows

A. Grooved Channel

Above a critical Reynolds number R_c, the flow becomes exponentially unstable to small disturbances. However, nonlinear effects stabilize the disturbance at some fixed amplitude. A stable solution of the nonlinear equations is found in the vicinity of the critical conditions for the onset of linear instability. The flow bifurcates from a steady-state to a time-periodic secondary self-sustained flow; this primary bifurcation occurs at $R_c = 320$ for the base grooved-channel geometry. The velocity exhibits an oscillatory behavior approaching a limit cycle as it is shown in Fig. 4, in a phase plane plot of v vs u. The phase shift between the two components of the oscillatory velocity induces a Reynolds stress $(-\rho u'v')$ responsible for the increase in momentum diffusion, converting energy from the basic mean flow to the oscillatory flow and sustaining it. The velocity power spectrum shows a dominant frequency that coincides with the Tollmien-Schlichting frequency corresponding to the least stable Orr-Sommerfeld mode for plane Poiseuille flow.[5]

Figures 5 and 6 show a sequence of instantaneous streamline plots during one period τ of self-sustained oscillation at $R = 400$ ($1.3\ R_c$) and $R = 700$ ($2.2\ R_c$) respectively. At slightly supercritical Reynolds number flows (see Fig. 5), there is no significant interaction between the groove and outer flows. However, the mixing as well as the amplitude of the oscillatory velocity and the waviness of the flow increase as the Reynolds number is increased. The mixing between the groove and bulk flow is clearly seen in the streamline pictures of Fig. 6 by the bulging of the groove vortex into the channel. The flow pattern and vortex ejection mechanism for these self-sustained supercritical flows show a very close resemblance with the one corresponding to subcritical grooved-channel excitation.[17] In the former, the flow achieves the oscillatory behavior naturally, whereas in the latter, the flow is modulated at the frequency of the least stable channel mode.

B. Communicating Channels

The critical Reynolds number for the two-dimensional primary instability is $R_c = 110$ for the basic communicating channels geometry. In order to quantify the destabilizing effect of the channel interactions, the bottom wall in the grooved-channel geometry is removed, which allows communication between two channels. It is found that the critical Reynolds number is reduced by a factor of three in the basic geometry, due to the destabilizing effect of the counter-rotating vortices as well as the interaction between channels.

The evolution of the flow structure in terms of the instantaneous velocity vectors is shown in Fig. 7, in a sequence of six time frames within one flow cycle ($0 \le t \le \tau$) for $R = 1.3R_c$. The flow is slightly supercritical, and there is weak interaction between the groove and channel flows. The two aligned counter-rotating vortices of the steady flow of Fig. 3 become now an unstable configuration, shifting their positions and strengths during one period of oscillation. In this two-vortex regime, one vortex becomes stronger and moves toward the downstream wall, dissipating rotational kinetic energy; then, the weaker vortex moves upstream and gives place to the now stronger, second vortex to follow the same pattern.

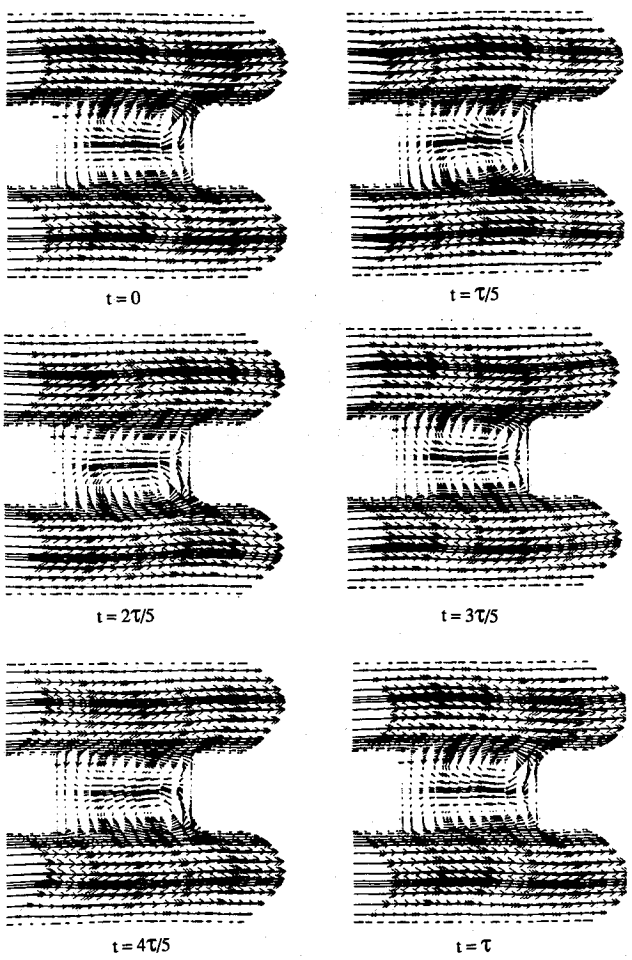

Fig. 7 Instantaneous velocity vectors at six times during one cycle of the self-sustained oscillatory flow at $R = 1.3\ R_c$ (two moving counter-rotating vortices are confined in the groove).

Taneda et al.[18] also found that two counter-rotating vortices constitute an unstable configuration in the cases of impulsive start of flow over a flat plate and a cylinder. Initially, a symmetrical pair of standing eddies is formed; though it will later breakdown into an oscillating vortex street despite the symmetric conditions. This, in turn, is indicative of a repulsive force experienced by the pair of vortices rotating in opposite directions. This force has the same origin as the attraction force existing between vortices rotating in the same direction, which results in the vortex-pairing process and roll-up found in free shear layers.[19]

For higher Reynolds number flows, the viscous forces are not strong enough to keep the vortices confined in the groove. A new flow regime is established in which the vortices in the groove are ejected alternatively to the upper and lower channels producing strong mixing between the groove and bulk flows.[16] The vortex-dynamics is synchronized with the wavy character of the flow which, indeed, corresponds to in-phase traveling Tollmien-Schlichting waves in both channels. As the Reynolds number is increased further, similar flow patterns are obtained, although the mixing is much stronger. The flow in the channel boundary layers becomes reversed and separates from the wall.

V. Heat-Transfer Results

In this section we present heat-transfer results for the grooved-channel geometry with uniform heat flux at the bottom wall and adiabatic conditions at the top wall and for the communicating channels with all surface uniformly heated. The Nusselt number is defined as the heat removed from the wall per unit temperature elevation,

$$Nu = \frac{q''_0 h}{k\overline{\Delta T}} \tag{9}$$

$$\overline{\Delta T} = \frac{\int_{\partial D_h} <\theta - \theta_b> d\ell}{\int_{\partial D_h} d\ell} \tag{10}$$

where ∂/D_h is the heated region and q''_0 is the heat flux from one groove periodicity length per channel divided by its projected area in the streamwise direction; for the grooved channel, $q''_0 = q''(L + 2a)/L$ and for communicating channels, $q''_0 = q''[2(L + a) - \ell]/L$. The periodic part of the mixed-mean temperature, defined at $x = 0$, is:

$$\theta_b = \frac{\int_{-1}^{1} <u(x=0,y,t)\cdot\theta(x=0,y,t)> d(y/h)}{\int_{-1}^{1} <u(x=0,y,t)> d(y/h)} \tag{11}$$

where $<\ >$ refers to a time average.

A. Heat Transfer in Grooved Channels

A broad range of augmentation schemes have been proposed to enhance convective heat transfer. In this work, we investigate supercritical heat-transfer enhancement and compare this technique with the following two methods of transport enhancement by flow destabilization 1) active flow modulation by imposing externally an oscillatory flow,[20] and 2) passive flow modulation by placing small cylindrical eddy promoters at the lip of the groove.[3,4] Our interest is to deter-

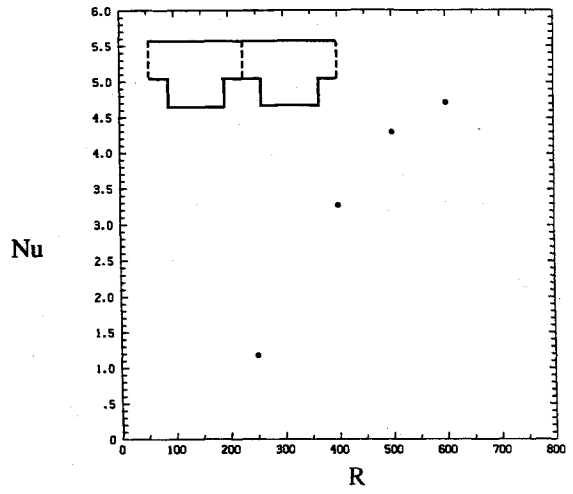

Fig. 8 Time- and space-averaged Nusselt number as a function of the Reynolds number for the self-sustained oscillatory grooved-channel flow. For highly unsteady laminar flows ($R = 600$), the heat transfer is increased by almost four times compared to the steady flow, $R = 250$.

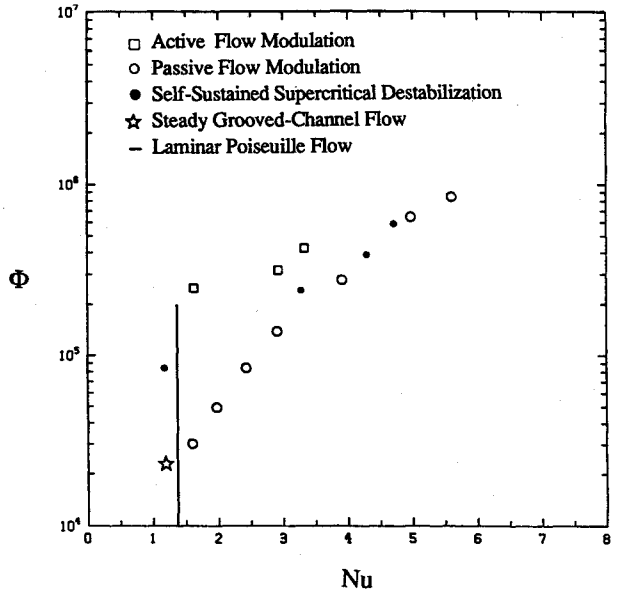

Fig. 9 Power dissipation Φ as a function of Nusselt number for grooved (□, ○, ●, *) and plane (–) channel flows. Heat flux is prescribed on the bottom wall, while the top wall is adiabatic.

mine which is the best enhancement technique as regards minimization of the power dissipation for a given Nusselt number.

We begin by calculating the steady-state heat-transfer characteristics to provide a baseline calculation to compare the effects of self-sustained oscillations on the heat transfer. The steady isotherms plots for $R = 250$ and $Pr = 1$ show a pattern corresponding to a recirculation flow in the groove region; the effect of the groove vortex does not extend to the channel part of the flow where the thermal solution is like that in a laminar fully developed plane-channel flow. The corresponding Nusselt number is $Nu = 1.18$ compared to $Nu = 1.35$ for the one-wall heated plane channel flow. This difference is due mainly to the increase in the conduction length associated with the groove depth.

The Nusselt number increases significantly for sufficiently supercritical flow because of the Reynolds flux generated by the unsteady motion. This is shown in Fig. 8, where the time- and space-averaged Nusselt number is plotted as a function of the Reynolds number. For $250 < R < 600$, the heat transfer augmentation is about fourfold compared to the steady grooved-channel flow solution. This implies that the Tollmien-Schlichting waves are good heat transporters and their natural excitation results in substantial enhancement of heat transport. Since not all systems are susceptible to supercritical destabilization, it is important to note the role of the groove geometric inhomogeneities. The grooves introduce periodic disturbances that closely match the least stable Tollmien-Schlichting wavelength, sustaining the oscillatory flow.

In active flow modulation, excitation of normally damped Tollmien-Schlichting waves is obtained by external modulatory forcing of the subcritical flow under resonant conditions. Greiner et al.[1] and Ghaddar et al.[20] found that resonant oscillatory forcing at 20% flow rate modulation of the otherwise subcritical flow results in doubling the heat-transfer coefficient in a particular grooved-channel geometry ($L/h = 6.66$, $\ell/h = 2.22$, $a/h = 1.11$). The enhancement parameter as a function of the forcing frequency is shown in Fig. 14 of Ref. 20, where a peak resonant augmentation in heat transfer is observed. A similar resonance phenomenon with transport enhancement is obtained by imposing an oscillatory flow on a cylinder at a frequency near the natural vortex shedding frequency (Fig. 4 of Ref. 2).

In passive flow excitation, small stationary cylinders are inserted in the grooved channel to act as flow excitors. The matching between the cylinder and channel flow patterns results in similar strong mixing of the flow.[3,4] Therefore, significant heat-transfer enhancement occurs as in the case of self-sustained oscillatory flows presented in this work, in which the groove inhomogeneity creates the flow structures that destabilize the channel Tollmien-Schlichting waves, even in the absence of the external forcing or passive flow modulation.

We compare next the three methods of heat transfer enhancement in grooved channels in terms of pumping power and Nusselt number, where the dimensionless pumping power is defined as

$$\Phi = \frac{3}{4} < \frac{dp}{dx} > \frac{Vh^4}{\rho\nu^3} \tag{12}$$

The power dissipation Φ as a function of the Nusselt number Nu for passive modulation, active modulation, and self-sustained oscillatory flow in grooved channels is shown in Fig. 9. In all systems, the Nusselt number increases significantly for sufficiently unstable flows. However, the optimal heat-transfer enhancement system regarding minimum power dissipation corresponds to the passive flow modulation by inserting eddy promoters. Although the friction losses due to the cylinder drag are not directly recoverable as heat-transfer enhancement, this system performs better mainly because the instabilities originated at the cylinder shear layers further destabilize the flow. Unsteady states at lower Reynolds number are achieved in this way. The critical Reynolds number is 125 compared with 320 for spontaneously occurring self-sustained oscillatory flows.[12]

At higher Nusselt numbers, flows with passive modulation and supercritical self-sustained oscillations are competitive. These augmentation methods have proven to be better than subcritical resonant heat-transfer augmentation not only in pumping power requirements but also because they are inherently more reliable, not requiring a precise frequency tuning, away from which almost no enhancement is obtained.

Experimental investigations of the performance of microgrooves and microcylinders in turbulent regime have been performed recently.[21,22] They suggest that flows should be stabilized at their naturally stable spatial scales of motion in order to achieve a better transport enhancement, i.e., global flow destabilization for laminar flows and viscous sublayer destabilization for turbulent flows.

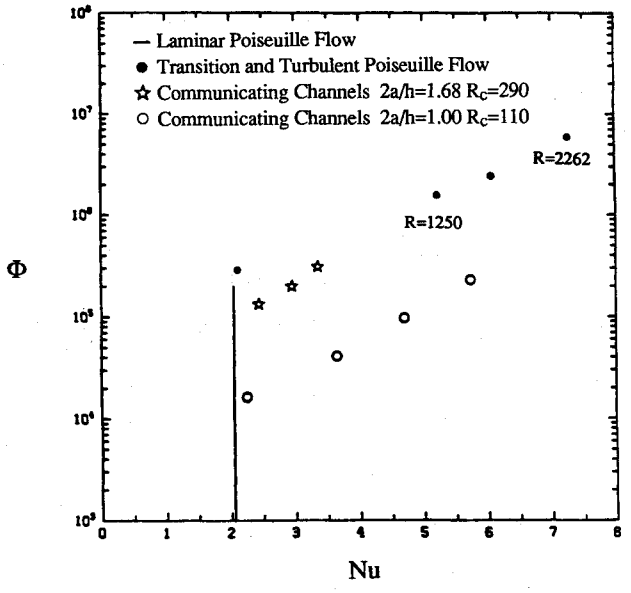

Fig. 10 Power dissipation Φ as a function of Nusselt number for the communicating channels (*, ○) and plane channel flows (●, –); heat flux is prescribed on all of the surfaces.

B. Heat Transfer in Communicating Channels

At the onset of large-scale mixing produced naturally at $R > R_c$ not only the heat transfer but also the pressure drop increases significantly. Traditionally, in the heat-transfer literature, it is the increase in pressure drop that is usually considered as a measure of the penalty associated with heat-transfer augmentation. However, another important measure is the pumping power (pressure drop times flow rate) since a more unstable system can achieve the same Nusselt number at a much lower Reynolds number, that is, at a smaller flow rate, although with a higher pressure drop. Therefore, in this work we consider the penalty in the pumping power as well as the enhanced heat-transfer coefficient to evaluate the overall performance of a system.

We now study the effect on the heat transfer of the spontaneously occurring, self-sustained oscillations in communicating channel flows and compare with the heat transfer in straight channel flows on an equal pumping power basis. Figure 10 shows the pumping power Φ as a function of Nusselt number Nu for the base geometry $L/h = 5$, $\ell/h = 3$ and for separation between communicating channels $2a/h = 1.0$ and $2a/h = 1.68$. The critical Reynolds number for these geometries are 110 and 290, respectively. In addition, data for laminar and turbulent flat channel flow[22] with both walls uniformly heated are indicated in Fig. 10. It is seen that at $\Phi = 2 \times 10^5$, the flat channel operates in the laminar regime and gives $Nu = 2.06$, whereas, the least stable communicating channels geometry yields $Nu = 5.76$. Therefore, the heat transfer is increased by almost three times for the same power dissipation in communicating channels flows compared to flat channel solutions.

The relatively thin boundary layers created by the interrupted surfaces, the large-scale mixing due to self-sustained laminar oscillations, and the communication between channels are the key factors on the high heat-transfer performance of these surfaces. The mixing in these flows is responsible for the heat-transfer enhancement as it is in turbulent flows. However, the ordered self-sustained oscillations in laminar supercritical flows have less viscous dissipation than the random, chaotic, fluctuation of turbulent flows, therefore requiring less pumping power to reach the same transport rates.

We now compare the power dissipation for the two communicating channels geometries with $R_c^o = 110$ and $R_c^* = 290$ in Fig. 10. To obtain $Nu \cong 2.25$, the pumping power required by the more unstable system Φ^o is approximately eight times smaller than the one required by the more unstable system Φ^*. The ratio between the pumping powers Φ^o/Φ^* is roughly the square of the ratio between the Reynolds numbers $(R^o/R^*)^2$. This numerical experiment verifies that Φ is proportional to $Nu \cdot R^2$ and a more unstable flow, i.e., a flow that achieves same Nusselt number at lower Reynolds number, requires less pumping power. This figure also shows that very well mixed, laminar self-sustained oscillatory flows require up to one order of magnitude less pumping power than turbulent plane channel flows to achieve the same transport rates.

The strong mixing induced by the self-sustained oscillations and the interaction between channels suggests that this augmentation scheme has potential for further application in viscous sublayer destabilization in turbulent flows. The geometric parameters in the communicating channels system must be chosen to guarantee, first, supercritical conditions and, second, a self-sustained oscillation frequency higher than the expected burst frequency. This could generate significant transport enhancement by

1) local mixing due to the self-sustained oscillation in the sublayer region in the time between consecutive bursts, and

2) promoting interchannel communication and allowing a single burst to affect both sides of the heated surface.

VI. Conclusions

Numerical simulations of separated flows in grooved and communicating channels show that above certain R_c, these flows exhibit laminar self-sustained oscillations at a frequency very close to the least stable channel frequency. These oscillatory flows not only increase significantly the transport rates but also are optimal as regards pumping power. The pumping power is proportional to the square of the Reynolds number for a given Nusselt number. Thus, reduction of a flow's critical Reynolds number increases its transport on an equal pumping power basis. An optimal heat-transfer system is equivalent to a more unstable system, i.e., a system with lower R_c for the onset of laminar oscillations.

The heat transfer increases as much as three times for the same power dissipation in supercritical communicating channels flows when compared to flat channel solutions. The heat-transfer effectiveness of these systems is due to the strong mixing produced by the self-sustained oscillations, the interaction between channels, and the decrease on the thermal resistance in the restarting boundary layers.

Large-scale mixing produced by spontaneous supercritical flow destabilization as well as the increase in the Reynolds and heat fluxes are responsible for the heat-transfer enhancement as it is in turbulent flows. However, ordered laminar self-sustained oscillations yield less viscous dissipation than the random, chaotic, turbulent fluctuations, therefore requiring less pumping power to reach the same transport rates.

Acknowledgments

This work was supported by a Venezuelan Council for Scientific and Technological Research (CONICIT) Fellowship (CHA); Cray-XMP computer time was provided by the Pittsburgh Supercomputing Center. These supports are greatly appreciated.

References

[1]Greiner, M., Ghaddar, N. K., Mikic, B. B., and Patera, A. T., "Resonant Convective Heat Transfer in Grooved Channels," *Proceedings of the Eigth International Heat Transfer Conference*, Vol. 6, 1986, p. 2867.

[2]Amon, C. H., Mikic, B. B., and Korin, E., "Effect of Oscillatory Flow on Heat Removal from Circular Fins," *Cooling Technology for Electronic Equipment*, Hemisphere, Washington, DC, 1988, p. 125.

[3]Karniadakis, G. E., Mikic, B. B., and Patera, A. T., "Heat Transfer Enhancement by Flow Destabilization: Application to the Cooling Chips," *Proceedings of the International Symposium on Cooling*

Technology for Electronic Equipment, 1987, p. 498.

[4]Ratts, E., Amon, C. H., Mikic, B. B., and Patera, A. T., "Cooling Enhancement of Forced Convection Air Cooled Chip Array through Flow Modulation Induced by Vortex-Shedding Cylinders in Cross-Flow," *Cooling Technology for Electronic Equipment*, Hemisphere, Washington, DC, 1988, p. 183.

[5]Amon, C. H., "Heat Transfer Enhancement and Three-Dimensional Transitional Flows by a Spectral Element-Fourier Method," Sc.D. Thesis, Massachusetts Institute of Technology, Cambridge, MA, 1988.

[6]Amon, C. H., and Patera, A. T., "Numerical Calculation of Stable Three-Dimensional Tertiary States in Grooved-Channel Flow," *Physics of Fluids* A, Vol. 1, No. 12, 1989, p. 2005.

[7]Squire, H. B., *Proceedings of the Royal Society of London*, Vol. A 142, 1933, p. 621.

[8]Arvizu, D. E., and Moffat, R. J., "Experimental Heat Transfer from an Array of Heated Cubical Elements on an Adiabatic Channel Wall," Stanford Univ., Palo Alto, CA, Rept. No. HMT-33, 1984.

[9]Cur, N., and Sparrow, E. M., "Experiments on Heat Transfer and Pressure Drop for a Pair of Colinear, Interrupted Plates Aligned Channel Wall," *International Journal of Heat and Mass Transfer*, Vol. 21, 1978.

[10]Yang, W., "Forced Convective Heat Transfer in Interrupted Compacted Surfaces," *Proceedings of the ASME-JSME Thermal Engineering Conference* 1983, p. 105.

[11]Reynolds, O., "On the Extent and Action of Heating Surface for Steam Boilers," *Proceedings of the Mancester Lit. Phil. Soc.*, Vol. 14, 1874.

[12]Karniadakis, G. E., Mikic, B. B., and Patera, A. T., "Minimum-Dissipation Transport Enhancement by Flow Destabilization: Reynolds' Analogy Revisited," *Journal of Fluid Mechanics*, Vol. 192, 1988, p. 365.

[13]Orszag, S. A., and Kells, L. C., "Transition to Turbulence in Plane Poiseuille and Plane Couette Flows," *Journal of Fluid Mechanics*, Vol. 96, 1980, p. 159.

[14]Patera, A. T., "A Spectral Element Method for Fluid Dynamics: Laminar Flow in a Channel Expansion," *Journal of Computational Physics*, Vol. 54, 1984, p. 468.

[15]Maday, T., and Patera, A. T., "In State of the Art Surveys in Computation Mechanics," ASME (to be published).

[16]Amon, C. H., and Mikic, B. B., "Flow Pattern and Heat Transfer Enhancement in Self-Sustained Oscillatory Flows," AIAA Paper 89-0428, Jan. 1989.

[17]Ghaddar, N. K., Korczak, K. Z., Mikic, B. B., and Patera, A. T., "Numerical Investigation of Incompressible Flow in Grooved-Channels, Part I," *Journal of Fluid Mechanics*, Vol. 163, 1986, p. 99.

[18]Van Dyke, M., "An Album of Fluid Motion," Parabolic, 1982.

[19]Winant, C. D., and Brownand, F. K., "Vortex Pairing: The Mechanism of Turbulent Mixing Layer Growth at Moderate Reynolds Numbers," *Journal of Fluid Mechanics*, Vol. 63, 1974, p. 237.

[20]Ghaddar, N. K., Magen, M., Mikic, B. B., and Patera, A. T., "Numerical Investigation of Incompressible Flow in Grooved-Channels; Part 2," *Journal of Fluid Mechanics*, Vol. 168, 1986, p. 541.

[21]Amon, C. H., Kozlu, H., and Karniadakis, G. E., "Hydrodynamic Stability and Scalar Transport in Wall Bounded Flows," *Bulletin of the American Physical Society*, Division of Fluid Dynamics, Vol. 32, No. 10, 1987, p. 2034.

[22]Kozlu, H., Mikic, B. B., and Patera, A. T., "Minimum Dissipation Heat Removal by Scale-Matched Flow Destabilization," *International Journal of Heat and Mass Transfer*, Vol. 31, 1988, p. 2023.